Research Square

Preprints are preliminary reports that have not undergone peer review.
They should not be considered conclusive, used to inform clinical practice,
or referenced by the media as validated information.

Microbial biomass and enzyme activities determine dynamics of soil organic carbon stocks and fractions along an age-sequence of Mongolian pine plantations

Yansong Zhang
De-Hui Zeng
https://orcid.org/0000-0002-3130-3050
Zeyong Lei
Xin Li
Guigang Lin (linguigang@126.com)
Institute of Applied Ecology Chinese Academy of Sciences https://orcid.org/0000-0003-4473-2708

Research Article

Keywords: Afforestation of sandy grassland, Mineral-associated organic carbon, Mineral sorption, Particulate organic carbon, Phenol oxidase, Soil acid-base chemistry

Posted Date: May 20th, 2022

DOI: https://doi.org/10.21203/rs.3.rs-1635102/v1

License: This work is licensed under a Creative Commons Attribution 4.0 International License.
Read Full License

Abstract

Purpose

Afforestation is increasingly recognized as an effective measure to mitigate elevated atmospheric carbon (C) dioxide and combat climate change. While afforestation can increase C sequestration by biomass production with tree growth, little is known about whether and how tree growth affects soil organic carbon (SOC) stocks and stability. Here, we aimed to explore mechanisms underlying changes in SOC stocks and fractions with stand development from the perspective of tree-microbe-mineral interactions.

Methods

We measured annual litter inputs, soil exchangeable base cations, microbial biomass, hydrolytic and oxidative enzymes, and SOC stocks and fractions along an age-sequence of Mongolian pine (*Pinus sylvestris* var. *mongolica*) plantations with six age classes ranging from 15- to 61-year-old and adjacent grasslands in the Keerqin Sandy Lands, Northeast China.

Results

We found that afforestation of grasslands did not significantly affect 0–100 cm SOC stocks. Ecosystem C stocks linearly increased with stand development, and this C accretion was mainly attributed to tree biomass C sequestration. Topsoil (0–10 cm soil layer) mineral-associated C (MAOC) stocks and phenol oxidase activities increased, and particulate organic C (POC) stocks and β-glucosidase activities decreased with increasing stand age, but these changes disappeared in the 61-year-old stand. Structural equation model revealed that topsoil MAOC stocks were directly related to microbial biomass and β-glucosidase and phenol oxidase activities, but not directly to exchangeable calcium concentrations. Moreover, topsoil POC stocks were directly related to β-glucosidase activities, but not directly to annual litter inputs.

Conclusions

Altogether, our findings suggest that soil microbes play a central role in mediating the dynamics of SOC stocks and stability along stand development.

Introduction

Climate change induced by anthropogenic activities has been considered as a great threat to ecosystem health, such that world-wide strategies to mitigate climate change are imperative (Lal 2004; Bonan 2008; Creutzig et al. 2018). Afforestation has been increasingly recognized as an effective measure to mitigate elevated atmospheric carbon (C) dioxide and combat climate change (Tong et al. 2018; Hong et al. 2020).

Under the action of this consensus, plantations are widely established at an annual increase rate of 1.4% and now account up to 7.2% of the global forest area (FAO 2020). Consequently, quantifying C sequestration capacity of these new forests and understanding mechanisms affecting this capacity are critical to evaluate the role of afforestation in climate change mitigation (Friggens et al. 2020; Wang and Huang 2020). Afforestation can indeed enable C sequestration by the production of tree biomass (Chen et al. 2021), yet whether and to what extent soils following afforestation contribute to C sequestration remain largely unclear.

Impacts of afforestation on soil organic C (SOC) stocks have received considerable attention, yet no consistent pattern is obtained. Previous studies have reported that afforestation has positive (Martens et al. 2004; Zhang et al. 2020), neutral (Ortiz et al. 2016; Wang et al. 2016) or even negative (Wiesmeier et al. 2009; Friggens et al. 2020) effects on SOC stocks. A key reason for these inconsistent and conflicting results may be because these studied plantations are at distinct development stages (Guo and Gifford 2002; Neumann-Cosel et al. 2011). In the early stage of stand development, SOC stocks usually decline owing to low litter inputs and to high nutrient demands of rapid tree growth that accelerate organic matter decomposition (Hiltbrunner et al. 2013; Chen et al. 2017). With stand development, SOC stocks gradually increase due to C inputs from aboveground litterfall, root exudates and root turnover outweighing C decomposition (Davis and Condron 2002; Hiltbrunner et al. 2013). In theory, when C inputs equilibrate with C outputs, a new steady state of SOC stocks can be reached at the later stage of afforestation (Bárcena et al. 2014). Therefore, studying SOC dynamics with plantation age is crucial to understand factors controlling SOC transformation and sequestration potential. However, most previous studies usually focus on short-term afforestation effects and thus the theoretically steady state of SOC stocks may not be determined, which constrains accurately evaluating the contribution of afforestation to SOC sequestration.

Apart from SOC stocks, SOC stability, reflecting the resistance of SOC to disturbance, is also considered as another important indicator to assess afforestation effects on climate change mitigation (Dungait et al. 2012). Theoretical and experimental studies suggest that the relative abundance of fast-turnover particulate organic C (POC) and slow-turnover mineral-associated organic C (MAOC) can be considered as a mechanistic indicator of SOC stability (Haddix et al. 2020; Lavallee et al. 2020). The POC mainly consists of partially decomposed plant residues and persists in soils via inherent biochemical recalcitrance, such that it is more susceptible to disturbance (Witzgall et al. 2021). In contrast, MAOC is predominantly made of microbial products and plant-derived dissolved organic matter (DOM) during the catabolism of POC, and persists in soils through chemical bonding to minerals (Sokol et al. 2019; Angst et al. 2021). Consequently, studying pool sizes and dynamics of these two C fractions is critical to understand mechanisms underlying afforestation effects on SOC accrual, persistence and response to environmental changes.

The POC and MAOC content can be influenced by stand development due to age-related variation in tree-microbe-mineral interactions (Almeida et al. 2021). With tree growth, litter production increases, and litter quality usually decreases characterized by high C:N ratios and lignin concentrations (Prescott and

Vesterdal 2021). Meanwhile, stand development may lead to soil acidification because the more recalcitrant litter produced in the older stands can produce greater organic acids during decomposition and the increase of base cation accumulation in biomass with tree growth can reduce soil acid-buffering capacity (Jobbágy and Jackson 2003). Considering that soil acid-base status is a key determinant of microbial growth and survival, stand development may affect microbial biomass, community composition and extracellular enzyme activities by soil acidification (Clemmensen et al. 2015; Yang et al. 2020). Thus, POC content may change with stand development because of age-related variation in litter quantity that determines C inputs and in microbial extracellular enzyme activities that affect C outputs (Xu et al. 2021). As the precursors of MAOC are mainly microbial necromass (the *in vivo* microbial turnover pathway) and DOM produced by enzymatic decomposition of plant litter (the *ex vivo* modification pathway; Liang et al. 2017), changes in soil microbial biomass and extracellular enzyme activities with tree growth could influence MAOC content (Shao et al. 2017). Additionally, the decrease in base cations (e.g. Ca^{2+}) and the increase in the solubility of Al^{3+} and Fe^{3+} associated with soil acidification can affect MAOC formation and stabilization (Clarholm and Skyllberg 2013). Specifically, the loss of Ca^{2+} can lead to the release of C adsorbed to minerals via disrupting polyvalent cation bridging (Rowley et al. 2018; Barreto et al. 2021). Conversely, increased Al^{3+} and Fe^{3+} solubility can improve MAOC content by forming complexes with C (Kleber et al. 2021). Therefore, litter quantity and quality, microbial biomass and activities, and soil geochemical properties co-determine responses of soil C fractions to stand development.

The primary objective of this study was to investigate how SOC stocks and stability changed with stand development, and to explore mechanisms underlying these changes from the perspective of tree-microbe-mineral interactions. To achieve this objective, we selected a chronosequence of Mongolian pine (*Pinus sylvestris* var. *mongolica*) stands planted on sandy grasslands with tree ages ranging from 15- to 61-year-old, and adjacent grasslands in Northeast China. All stands and grasslands are on fairly flat ground and the maximum distance between each other is less than 10 km, such that our experimental design could largely eliminate the confounding effects of climate and soil parent materials. We measured litter quantity and quality, soil exchangeable base cations, microbial biomass, hydrolytic and oxidative enzymes, and SOC, POC and MAOC stocks. Based on these measurements, the following hypotheses were tested: (1) SOC stocks would decrease at the early stage of afforestation, but gradually increase and eventually surpass the level of grassland SOC stocks with stand development; (2) POC stocks would increase with stand development because of the increase in litter quantity and the decrease in litter quality with tree growth; (3) stand development would increase MAOC stocks, since the increase in microbial biomass and enzyme activities with tree growth can transform more plant- to microbial-derived C.

Materials And Methods

Study site and experimental design

Our study was conducted at the Research Institute of Sand Control and Utilization, located in the southeast of Keerqin Sandy Lands, Liaoning Province, Northeast China (42°42' N, 122°29' E, 225 m a.s.l.). This study site has a temperate continental monsoon climate, with mean annual temperature of 7.7 ℃, mean annual precipitation of 474 mm and mean annual evaporation of 1580 mm. According to the US Soil Taxonomy, soil in our study site is classified as the Typic Ustipsamment developed from eolian parent materials (Chen et al. 2010). Soil is coarse textured consisting of 95.6% sand, 4.1% silt and 0.3% clay, and is nutrient poor with SOC of 3.46 $g \cdot kg^{-1}$ and total nitrogen (N) of 0.20 $g \cdot kg^{-1}$ in the 0–10 cm soil layer. The native vegetation is sandy grasslands dominated by *Cleistogenes squarrosa*, *Eragrostis pilosa* and *Elymus dahuricus*. For the purpose of fixing sand dunes and reducing wind erosion, Mongolian pine has been introduced for afforestation in our study site since 1950s.

A space-for-time substitution was used to investigate the long-term effect of stand development on SOC stocks and stability. We selected a chronosequence of Mongolian pine stands with six age classes (15-, 19-, 33-, 40-, 51-, and 61-year-old) and adjacent sandy grasslands in August 2020. All plantation stands were established on sandy grasslands by planting two-year-old seedlings in 40 cm × 40 cm × 40 cm pits with a spacing of 2 m × 5 m. These stands received no management practices, except that they were thinned twice between 15- and 33-year-old. For each age class, five stands were selected and a 20 m × 20 m plot was established in each stand. The distance between stands of the same age is at least 0.2 km to enable stands to be treated as independent replicates, and all stands are on fairly flat ground (a slope of less than 2°) and within 10 km to avoid confounding effects of climate and soil parent materials. Five 5 m × 5 m grassland plots were established at about 50 m distance from the plantation stand edge.

Soil and litter sampling

In August 2020, tree height and diameter at breast height (DBH, 1.3 m) were measured for all individuals in plantation plots. In each plantation and grassland plot, five soil cores were collected using a 2.5-cm diameter stainless steel corer from depths of 0–10, 10–20, 20–40, 40–60, 60–80, and 80–100 cm. Soil cores from the same plot were pooled together, sieved through a 2-mm mesh to remove rocks and roots, and then placed into a cooler, transported to the laboratory and processed immediately. Soil samples for measuring enzyme activities were immediately processed, for measuring organic C, N and acid-base chemistry were air-dried, and for measuring phospholipid fatty acid (PLFA) were stored at -80 ℃. In each plot, three soil samples of each soil layer were collected using 5-cm diameter volumetric rings to determine bulk density. For each plantation plot, annual litter input was determined by collecting litter samples from three randomly selected 50 cm × 50 cm subplots at the end of litterfall period in late-November 2020. Litter samples from these three subplots were pooled together, and freshly senesced litter was picked out and weighed after drying at 65 ℃ to constant mass. Litter samples were ground to pass a 0.25-mm mesh to measure C and N concentrations.

Soil chemical and biological analyses

For soil and litter samples, organic C concentration was determined using the $K_2Cr_2O_7$-H_2SO_4 oxidation method (Lefroy et al. 1993), and total N concentration was determined by a continuous-flow autoanalyzer (AutoAnalyzer III, Bran + Luebbe GmbH, Germany) after digested by the Kjeldhl method (Kirk 1950). Soil pH of 0–10 and 10–20 cm soil layers was measured in slurry of 25 ml distilled water and 10 g air-dried soils using a bench-top electrode pH meter. For determining exchangeable base cations, 10 g air-dried soil was extracted with 50 ml of 1 M ammonium acetate solution, shaken for 30 minutes, centrifuged and then filtered. Filtrate was analyzed to measure exchangeable Ca^{2+}, Mg^{2+}, K^+ and Na^+ concentrations by an inductively coupled plasma-optical emission spectrometry (5100 ICP-OES, Agilent Technologies, Santa Clara, USA). Exchangeable bases were calculated as the sum of exchangeable Ca^{2+}, Mg^{2+}, K^+ and Na^+ concentrations.

Soil organic C was separated into particulate organic carbon (POC) and mineral-associated organic carbon (MAOC) by a size fractionation procedure (Cambardella and Elliott 1992). Briefly, 10 g air-dried soil was dispersed with 100 ml of 5 $g \cdot L^{-1}$ sodium hexametaphosphate, shaken at 90 rpm and 18 ℃ for 18 hours on a homothermal shaker. After that, soil slurry was sieved through a 53-μm sieve and repeatedly washed using deionized water. The POC fraction that retained on the sieve was transferred into aluminum dishes, weighed after drying at 60 ℃ to constant mass, ground, and then analyzed for C concentration. The MAOC stock was calculated as differences between SOC and POC stocks.

Potential activities of four C-degrading enzymes in 0–10 and 10–20 cm soil layers were determined by the colorimetric method (Eivazi and Tabatabai 1988; Deng and Tabatabai 1994; Dick 2011). For β-glucosidase (BG) activity, 5 g fresh soil was incubated at 37 ℃ for 1 hour with 20 ml MUB buffer (pH = 6.0) and 5 ml of 25 mM *p*-nitrophenol glucopyranoside, after which 5 ml of 0.5 M $CaCl_2$ and 20 ml of Tris buffer (pH = 12.0) were added to terminate the reaction. The product, *p*-nitrophenol, was measured at 400 nm with a spectrophotometer (UV-1750, Shimadzu, Kyoto, Japan). For cellobiohydrolase (CBH) activity, 10 g fresh soil was incubated at 37 ℃ for 72 hours with 1.5 ml methylbenzene, 5 ml of 1% sodium carboxymethyl cellulose and 5 ml acetate buffer (pH = 5.5). Soil suspension was thoroughly shaken and filtered, after which the product, glucose, was measured at 540 nm with the spectrophotometer. For phenol oxidases (POX) and peroxidase (PER) activities, 0.5 g fresh soil was incubated at 25 ℃ for 30 minutes with 3 ml acetate buffer (pH = 5.0) and 2 ml L-3,4-dihydroxyphenylalanine (L-DOPA) in the presence and absence of 0.2 ml of 0.3% H_2O_2, after which soil suspension was centrifuged at 5 ℃ for 5 minutes and then filtered. The product, dopachrome, was measured at 475 nm with the spectrophotometer. The POX activity is indicated by the L-DOPA metabolism in the absence of H_2O_2, and PER activity is calculated as the difference in L-DOPA metabolisms between the presence and absence of H_2O_2.

Soil microbial biomass and community structure in the 0–10 cm soil layer were determined by measuring phospholipid fatty acids (PLFA) (Bossio and Scow 1998; Lin et al. 2020). Briefly, freeze-dried soil was extracted by the mixture of methanol, chloroform and citrate buffer. Extracted lipids were divided into phospholipids, neutral lipids and glycolipids on silicic acid columns. After that, phospholipids were

methylated and measured by a gas chromatograph equipped with a flame ionization detector (Agilent 6890 N, Santa Clara, CA, USA). The PLFAs were quantified by adding methyl nonadecanoate fatty acids as the internal standard. The PLFAs of i14:0, i15:0, a15:0, i16:0, 16:1ω7c, i17:0, a17:0, cy17:0, 18:1ω7c and cy19:0 were used as biomarkers of soil bacteria, and 18:2ω6,9c as the fungal biomarker (Angst et al. 2019). Fungal:bacterial (F:B) ratio was calculated as the ratio of fungal PLFAs to bacterial PLFAs.

Calculations and statistical analyses

Biomass of tree components (i.e. stem, branch, foliage and root) was calculated using the following allometric equations:

$$M = a \times DBH^{b} \times Y^{c}$$

where M is biomass of tree components, DBH is the diameter at breast height and Y is the tree age. Parameters of *a*, *b* and *c* shown in Table S1 were obtained from Zhang et al. (2019), which measured biomass accumulation of Mongolian pine plantations with tree ages ranging from 12- to 58-year-old in our study site. Biomass C (BC; kg) of tree components was calculated as follows:

$$BC = M \times (m \times Y + n) \times 0.01$$

where *m* and *n* parameters shown in Table S1 are obtained from Jia et al. (2012). Total tree biomass C (TBC; kg) was the sum of the tree components biomass C. Tree biomass C stock (TBC_{stock}; Mg ha^{-1}) was calculated as follows:

$$TBC_{stock} = 0.025 \times \sum_{i=1}^{n} TBC_{i}$$

where *n* is the number of Mongolian pines in a given plot. Total soil organic C stock (SOC_{stock}; Mg ha^{-1}) was calculated as follows:

$$SOC_{stock} = \sum_{i=1}^{6} (SOC_{i} \times BD_{i} \times T_{i})$$

where SOC_i, BD_i and T_i are the C concentration, bulk density and thickness of the *i*th soil layer, respectively.

All data were tested for normality by the Shapiro-Wilk test and for variance homogeneity by the Levene's test. If data did not meet the normality and variance homogeneity, they were log_{10}-transformed prior to analyses. One-way analysis of variance was conducted to analyze how stand characteristics, SOC stocks and fractions, soil acid-base chemistry, microbial biomass and enzyme activities changed along the chronosequence of Mongolian pine plantations. Post-hoc mean comparisons were evaluated by the least

significant difference. These analyses were performed using the SPSS 20.0 (SPSS Inc., Chicago, IL, USA), and the significant level was set at $\alpha = 0.05$.

Structural equation model was conducted using the lavaan package in R (Rosseel 2012) to analyze the direct and indirect effects of stand ages, litter quality and quantity, soil acid-base chemistry, soil microbial properties, and C fractions on SOC stocks in the 0–10 cm soil layer. The hypothesized relationships are that SOC stocks are determined by C fractions, which are mediated by stand development through affecting litter quality and quantity, soil acid-base chemistry and soil microbial properties (Fig. S1). In this model, litter quality and quantity are indicated by litter C:N ratio and annual litter C input, respectively. Soil microbial properties are indicated by total PLFAs, F:B ratio, and potential activities of BG, CBH, PER and POX (Fig. S1). Final structural equation model was obtained by stepwise removing paths with the highest probability value until all remaining paths were significant (i.e. $P < 0.05$). Fitness of structural equation model was evaluated by the Chi-square (χ^2) test, standardized root mean square residual (SRMR) and comparative fit index (CFI).

Results

Stand characteristics

Tree height and DBH showed a similar increasing pattern with increasing stand age (Table 1). Specifically, Mongolian pines exhibited rapid growth before 33-year-old and slow growth after that age. Annual litter C input increased from 2.47 Mg ha^{-1} yr^{-1} at age 15 to 2.80 Mg ha^{-1} yr^{-1} at age 40, and then decreased to 1.55 Mg ha^{-1} yr^{-1} at age 61 (Table 1). Litter C:N ratio initially decreased and subsequently increased with increasing stand age (Table 1). Tree biomass C stocks ranged from 20.22 to 43.22 Mg ha^{-1} and significantly increased with increasing stand age (Fig. 1a).

Table 1
Stand characteristics of Mongolian pine plantations.

Stand age (yrs)	Stand density (trees ha^{-1})	Mean height (m)	DBH (cm)	Annual litter C input (Mg ha^{-1} yr^{-1})	Litter C:N ratio
15	1105 (62)^{a}	4.21 (0.28)^{d}	8.76 (0.34)^{d}	2.47 (0.53)^{ab}	145.00 (8.29)^{a}
19	550 (146)^{b}	6.44 (0.73)^{c}	14.26 (1.93)^{c}	1.81 (0.47)^{bc}	108.75 (14.06)^{bc}
33	355 (80)^{c}	10.53 (0.62)^{b}	21.37 (1.52)^{b}	2.41 (0.40)^{abc}	105.75 (11.62)^{bc}
40	405 (54)^{c}	10.60 (2.24)^{b}	20.82 (3.32)^{b}	2.80 (1.07)^{a}	101.50 (13.43)^{c}
51	415 (101)^{c}	11.27 (1.31)^{b}	21.12 (1.40)^{b}	1.68 (0.45)^{cd}	104.50 (2.65)^{bc}
61	360 (72)^{c}	12.87 (1.11)^{a}	24.86 (1.21)^{a}	1.55 (0.29)^{d}	118.20 (13.26)^{b}

*Different lowercase letters indicate significant differences among stand ages. Values are means with SD in parentheses (n = 5). DBH, diameter at breast height.

SOC stocks and fractions

Across the six soil layers, stand age significantly affected SOC stocks in the 0–10 cm (Fig. 2a) and 80–100 cm (Fig. S2d), but not in the10–20 cm, 20–40 cm, 40–60 cm and 60–80 cm soil layers (Fig. S2a–S2c). In the 0–10 cm soil layer, SOC stocks slightly decreased after afforestation from 5.52 Mg ha^{-1} of grasslands to 4.44 Mg ha^{-1} of 15-year-old pine stands, but rapidly recovered with stand development and reached to 8.30 Mg ha^{-1} in 51-year-old pine stands (Fig. 2a). Afforestation significantly increased SOC stocks in the 80–100 cm soil layer from 3.74 Mg ha^{-1} of grasslands to 7.24 Mg ha^{-1} of 33-year-old pine stands (Fig. S2d). Total SOC stocks (i.e. 0–100 cm SOC stocks) did not significantly change along stand development (Fig. S2e). In contrast, ecosystem C stocks (i.e. the sum of total SOC and tree biomass C stocks) significantly increased with increasing stand age (Fig. 1b).

Stand age significantly influenced POC stocks in all six soil layers and the whole soil profile (i.e. 0–100 cm). In the 0–10 cm soil layer, POC stocks significantly decreased after afforestation from 0.71 Mg ha^{-1} of grasslands to 0.25 Mg ha^{-1} of 51-year-old pine stands, but increased to 1.42 Mg ha^{-1} in 61-year-old pine stands (Fig. 2b). For other five soil layers and the whole soil profile, afforestation initially increased

POC stocks and subsequently decreased POC stocks, with the lowest value in 40-year-old pine stands (Fig. S3). Stand development significantly affected MAOC stocks in the 0–10 cm soil layer (Fig. 2c) but not in other five soil layers and the whole soil profile (Fig. S4). In the 0–10 cm soil layer, MAOC stocks initially increased with increasing stand age and reached the highest value in 51-year-old stands, but subsequently decreased to the same level as grasslands in 61-year-old pine stands (Fig. 2c). Stand age had significant effects on POC:MAOC ratios in the whole soil profile and all soil layers except the 80–100 cm soil layer (Fig. 2d, Fig. S5).

Soil acid-base chemistry and microbial properties

Stand age significantly influenced soil pH in 0–10 and 10–20 cm soil layers and exchangeable bases in the 10–20 cm soil layer, but not other four acid-base chemical variables (Fig. 3). Specifically, stand development significantly reduced soil pH in the 0–10 cm soil layer with the lowest value in 40-year-old pine stands (Fig. 3a). In the 10–20 cm soil layer, soil pH (Fig. 3a) and exchangeable bases (Fig. 3b) initially decreased but rapidly recovered with increasing stand age.

In the 0–10 cm soil layer, stand development significantly influenced BG (Fig. 4a), CBH (Fig. 4b) and POX (Fig. 4c) activities. The 19- and 40-year-old pine stands had significantly greater BG activities than 33- and 61-year-old pine stands (Fig. 4a). The CBH activity was significantly higher in 19- and 40-year-old pine stands than 15- and 33-year-old pine stands (Fig. 4b). The 51-year-old pine stands had significantly greater POX activities than other age classes (Fig. 4c). In the 10–20 cm soil layer, BG (Fig. 4a) and PER (Fig. 4d) activities were significantly affected by stand development. Stand development significantly reduced BG activities (Fig. 4a). The PER activity initially increased but subsequently decreased with increasing stand age (Fig. 4d).

In the 0–10 cm soil layer, total PLFAs (Fig. 5a) and bacterial PLFAs (Fig. 5c) did not significantly change along stand development. Fungal PLFAs (Fig. 5b) and F:B ratios (Fig. 5d) showed the similar trend with increasing stand age. Stand development initially decreased fungal PLFAs and F:B ratios to the lowest values in 40-year-old pine stands, but subsequently increased them.

Factors affecting SOC stocks and fractions

The final structural equation model was well supported by our data (χ^2 = 68.49, P = 0.14, CFI = 0.92, SRMR = 0.15) and separately explained 22%, 65% and 90% of variation in POC, MAOC and SOC stocks (Fig. 6). The SOC stock was positively related to POC (β = 0.23, P < 0.01) and MAOC stocks (β = 0.99, P < 0.01). The POC stock was negatively related to BG activities (β = -0.46, P < 0.01). The MAOC stock was positively correlated with total PLFAs (β = 0.30, P = 0.02), and BG (β = 0.29, P = 0.02) and POX (β = 0.61, P < 0.01) activities (Fig. 6). Total PLFAs were positively related to exchangeable Ca^{2+} concentration (β = 0.44, P = 0.02), and POX activity was negatively related to litter C:N ratio (β = -0.52, P < 0.01) and positively to exchangeable Ca^{2+} concentration (β = 0.43, P < 0.01). The BG activity was positively correlated with annual litter C input (β = 0.44, P = 0.01) and exchangeable Ca^{2+} concentration (β = 0.36, P

= 0.03), and negatively with soil pH (β = -0.36, P = 0.04). Moreover, stand age negatively affected litter C:N ratio (β = -0.43, P = 0.02), annual litter C input (β = -0.60, P < 0.01) and soil pH (β = -0.38, P = 0.04; Fig. 6).

Discussion

Changes in SOC stocks and fractions along stand development

After 61 years of afforestation, Mongolian pine plantations had the similar level of total SOC stocks (i.e. 0–100 cm SOC stocks) to sandy grasslands (Fig. S2e). This result was consistent with regional and global meta-analyses showing that afforestation of grasslands had no significant effect on SOC stocks (Guo and Gifford 2002; Bárcena et al. 2014). Former land use is suggested as a critical determinant of afforestation effects on SOC stocks (Bárcena et al. 2014). Compared with cultivated, degraded or eroded ecosystems that usually become SOC sinks after afforestation (Martens et al. 2004; Zhang et al. 2020), afforestation of healthy and native ecosystems such as grasslands had no positive effects on SOC stocks or even resulted in SOC losses (Hu et al. 2008; Chen et al. 2010; Hiltbrunner et al. 2013). Moreover, inconsistent with our initial hypothesis, we did not find the decrease of SOC stocks in the 15-year-old stand relative to sandy grasslands (Fig. S2e). This result may indicate the rapid recovery of SOC stocks after afforestation in our study site, considering that SOC losses usually occur at the early stage of plantation establishment owing to the disturbance during planting (Don et al. 2009; Huang et al. 2011).

Our results showed that ecosystem C stocks linearly increased with stand development, and this C accretion was mainly attributed to tree biomass C sequestration (Fig. 1). In contrast, total SOC stocks did not significantly change along stand development (Fig. S2e). This result is consistent with other sandy land afforestation studies exhibiting that tree biomass rather than soil is the major contributor to ecosystem C accretion (Richter et al. 1999; Hu et al. 2008). The non-significant response of total SOC stocks to stand development in sandy lands may be because sandy soils ensure macroporosity and a highly oxidized environment that lead to high C mineralization rates (Richter et al. 1999). Compared with fine textured soils, coarse-textured soils have less potential to physically protect SOC from microbial attack (Chen et al. 2010; Haddix et al. 2020). Moreover, the nutrient-poor condition of sandy soils could limit soil organic matter accumulation. This is because high nutrient demands with rapid tree growth could accelerate organic matter decomposition to meet nutrient requirements, especially for tree species associating with ectomycorrhizal fungi that have high nutrient mining capacities (Wiesmeier et al. 2009; Terrer et al. 2021).

Unlike total SOC stocks, topsoil (i.e. 0–10 cm soil layer) SOC stocks significantly increased with increasing stand age (Fig. 2a), indicating the more responsiveness of topsoil than deeper layers to stand development (Poeplau and Don 2013; Shi et al. 2013). Separating SOC into multiple fractions with different formation and persistence is suggested as an efficient way to understand mechanisms underlying SOC dynamics with stand development (Lavallee et al. 2020; Lugato et al. 2021). Our results showed that the topsoil C accretion was primarily attributed to the positive effect of stand development on MAOC stocks, which accounted for 89% of SOC stocks in the topsoil (Fig. 2c–2d). Conversely, POC

stocks generally declined with increasing stand age but with an abrupt increase in the 61-year-old stand (Fig. 2b). The high proportion of MAOC stocks in old stands indicates the increase in SOC stability with stand development, since MAOC is less susceptible to disturbance than POC (Lavallee et al. 2020). However, the abrupt decrease in topsoil MAOC stocks, annual litter input (Table 1) and enzyme activities (Fig. 4) in the 61-year-old stand may suggest the decline in soil C sequestration potential in over-mature Mongolian pine plantations.

Changes in soil acid-base chemistry along stand development

Our results showed that with increasing stand age, soil pH and exchangeable bases decreased until 40-year-old, but subsequently recovered (Fig. 3a–3b). The increase in soil acidification with stand development may be due to the accumulation of base cations in tree biomass that reduce soil acid-buffering capacity (Jobbágy and Jackson 2003). Additionally, coniferous plantations can acidify soils through the production of organic acids during litter decomposition and the exudation of organic acids by roots (Alfredsson et al. 1998). The subsequent recovery of soil acid-base status in the 51- and 61-year-old stands may be because the increase in depth of vertical root distribution with tree growth can pump more base cations from the deep to surface soils (Dijkstra and Smits 2002; Jobbágy and Jackson 2004). Another explanation for this recovery may be the degradation of Mongolian pine plantations over 40-year-old, which can be evidenced by the abrupt decline in annual litter inputs (Table 1). Moreover, another study conducted in our study site also revealed the increasing loss of stem hydraulic conductivity when Mongolian pines are older than 40 years (Liu et al. 2018). This degradation can reduce the production of organic acids by roots and base-cation accumulation by tree growth, which may contribute to the recovery of soil acid-base status.

Soil acid-base chemistry is suggested as an important factor that regulates soil geochemical and microbial properties, which could further influence SOC formation and persistence (Clarholm and Skyllberg 2013). In neutral soils such as our study site, exchangeable Ca^{2+} plays important roles in forming MAOC through polyvalent cation bridging, which can protect C from microbial attack (Rowley et al. 2018; Kleber et al. 2021). However, our result showed that exchangeable Ca^{2+} concentration was not directly related to topsoil MAOC stocks (Fig. 6). This result may indicate that Ca^{2+} is not a limiting factor for MAOC formation when it acts as binding mediums for dissolved organic matter and mineral surfaces. In contrast, our result revealed that Ca^{2+} had significant indirect effects on topsoil POC and MAOC stocks by affecting microbial biomass and enzyme activities (Fig. 6). An explanation for this result may be that Ca is an essential constituent of microbial cell walls and plays important regulatory and metabolic functions in microbial cells (Dominguez 2004; Berg et al. 2017).

Microbial activity determines SOC dynamics along stand development

High plant C inputs alone are suggested to be insufficient to achieve large SOC stocks, and instead the efficiency of SOC formation and the degree of SOC stabilization are considered as the key determinant of SOC stocks (Dungait et al. 2012; Haddix et al. 2020). Microbial processing of plant-derived C and

biosynthesis is suggested to be important in SOC formation and stabilization (Liang et al. 2017; Sokol et al. 2019). Consistent with this viewpoint, our result showed that topsoil MAOC stocks were positively related to total PLFAs and BG and POX activities, and that total POC stocks were negatively related to BG activities (Fig. 6). The positive relationship between total PLFAs and MAOC stocks may be because some proportion of C in MAOC is microbial-derived including microbial necromass and metabolites, which can be absorbed to mineral surfaces forming organo-mineral complexes (Kallenbach et al. 2016; Fan et al. 2021). Indeed, Liang et al. (2019) estimated that microbial necromass can account for about 30% of SOC stocks in temperate forest soils by synthesizing global amino sugar data. Consequently, high microbial biomass may accompany with great microbial necromass and metabolites, which can improve MAOC stocks.

Apart from microbial-derived C, another important C source in MAOC is plant compounds that are partially oxidized and mobilized by microbial extracellular enzymes (Castellano et al. 2015; Liang et al. 2017; Sokol et al. 2019). Plant-derived compounds such as phenolic acids, lignin monomers and simple sugars can be directly absorbed by mineral surfaces forming MAOC (Sokol et al. 2019). This *ex vivo* modification pathway is suggested to play important roles in MAOC formation in nutrient-poor soils or some bulk soils with low microbial density (Liang et al. 2017; Sokol et al. 2019). This viewpoint was supported by our finding of the positive relationship between MAOC stocks with BG and POX activities (Fig. 6). Moreover, the tighter relationship of MAOC stock with POX activity than that with BG activity (Fig. 6) may be because compounds from lignin degradation driven by POX have stronger sorptive affinity with mineral surfaces than those from polysaccharide hydrolysis driven by BG (Sokol et al. 2019). The negative effect of BG activities on POC stocks (Fig. 6) may be because high BG activities can increase the decomposition of POC which is primarily made of plant residues (Haddix et al. 2020). The opposite effect of enzyme activities on POC and MAOC stocks suggests their double-edged sword effect on SOC stocks.

Conclusions

Along an age-sequence of Mongolian pine plantations, we examined mechanisms underlying changes in SOC stocks and fractions with stand development from the perspective of tree-microbe-mineral interactions. We showed that ecosystem C stocks linearly increased with stand development, and this C accretion was mainly attributed to tree biomass C sequestration. Topsoil MAOC stocks and POX activities increased, and POC stocks and BG activities decreased with increasing stand age, but these changes disappeared in the 61-year-old stand. Structural equation model revealed that topsoil MAOC stocks were positively related to total PLFAs and BG and POX activities, and topsoil POC stocks were negatively related to BG activities. Collectively, our findings suggest that soil microbial biomass and enzyme activities play a central role in mediating dynamics of SOC stocks and stability along stand development.

Declarations

Acknowledgements

We are grateful to the Research Institute of Sand Control and Utilization for providing the experimental site and relevant supports. This work was supported by the National Natural Science Foundation of China (Nos. 31700538, 31870603 and 31830015) and the Youth Innovation Promotion Association CAS (No. 2019200).

Author contributions

YZ, GL and DZ conceived this study; YZ, ZL and XL collected and analyzed that data. All authors contributed critically to the drafts and gave final approval for publication.

Data availability

The datasets generated during and/or analysed during the current study are available from corresponding authors on reasonable request.

Competing Interest

The authors declare that they have no known competing financial interests or personal relationships that could have appeared to influence the work reported in this paper.

References

1. Alfredsson H, Condron LM, Clarholm M, Davis MR (1998) Changes in soil acidity and organic matter following the establishment of conifers on former grassland in New Zealand. For Ecol Manage 112:245–252. https://doi.org/10.1016/S0378-1127(98)00346-6
2. Almeida LFJ, Souza IF, Hurtarte LCC, Teixeira PPC, Inagaki TM, Silva IR, Mueller CW (2021) Forest litter constraints on the pathways controlling soil organic matter formation. Soil Biol Biochem 163:108447. https://doi.org/10.1016/j.soilbio.2021.108447
3. Angst G, Mueller KE, Nierop KGJ, Simposn MJ (2021) Plant- or microbial-derived? A review on the molecular composition of stabilized soil organic matter. Soil Biol Biochem 156:108189. https://doi.org/10.1016/j.soilbio.2021.108189
4. Angst Å, Harantová L, Baldrian P, Angst G, Cajthaml T, Straková P, Blahut J, Veselá H, Frouz J (2019) Tree species identity alters decomposition of understory litter and associated microbial communities: a case study. Biol Fert Soils 55:525–538. https://doi.org/10.1007/s00374-019-01360-z
5. Bárcena TG, Kiaer LP, Vesterdal L, Stefánsdóttir HM, Gundersen P, Sigurdsson BD (2014) Soil carbon stock change following afforestation in Northern Europe: a meta-analysis. Glob Change Biol 20:2393–2405. https://doi.org/10.1111/gcb.12576
6. Barreto MSC, Elzinga EJ, Ramlogan M, Rouff AA, Alleoni LRF (2021) Calcium enhances adsorption and thermal stability of organic compounds on soil minerals. Chem Geol 559:119804. https://doi.org/10.1016/j.chemgeo.2020.119804

7. Berg B, Johansson M, Liu C, Faituri M, Sanborn P, Vesterdal L, Ni X, Hansen K, Ukonmaanaho L (2017) Calcium in decomposing foliar litter – A synthesis for boreal and temperate coniferous forests. For Ecol Manage 403:137–144. https://doi.org/10.1016/j.foreco.2017.08.022
8. Bonan GB (2008) Forests and climate change: Forcings, feedbacks, and the climate benefits of forests. Science 320:1444–1449. https://doi.org/10.1016/j.catena.2021.105694
9. Bossio DA, Scow KM (1998) Impacts of carbon and flooding on soil microbial communities: Phospholipid fatty acid profiles and substrate utilization patterns. Microb Ecol 35:265–278. https://doi.org/10.1007/s002489900082
10. Cambardella CA, Elliott ET (1992) Particulate soil organic-matter changes across a grassland cultivation sequence. Soil Sci Soc Am J 56:777–783. https://doi.org/10.2136/sssaj1992.03615995005600030017x
11. Castellano MJ, Mueller KE, Olk DC, Sawyer JE, Six J (2015) Integrating plant litter quality, soil organic matter stabilization, and the carbon saturation concept. Glob Change Biol 21:3200–3209. https://doi.org/10.1111/gcb.12982
12. Chen F, Zeng D, Fahey TJ, Liao P (2010) Organic carbon in soil physical fractions under different-aged plantations of Mongolian pine in semi-arid region of Northeast China. Appl Soil Ecol 44:42–48. https://doi.org/10.1016/j.apsoil.2009.09.003
13. Chen L, Wang H, Yu X, Zhang W, Lü X, Wang S (2017) Recovery time of soil carbon pools of conversional Chinese fir plantations from broadleaved forests in subtropical regions, China. Sci Total Environ 587–588:296–304. https://doi.org/10.1016/j.scitotenv.2017.02.140
14. Chen Y, Feng X, Tian H, Wu X, Gao Z, Feng Y, Piao S, Lv N, Pan N, Fu B (2021) Accelerated increase in vegetation carbon sequestration in China after 2010: A turning point resulting from climate and human interaction. Glob Change Biol 27:5848–5864. https://doi.org/10.1111/gcb.15854
15. Clarholm M, Skyllberg U (2013) Translocation of metals by trees and fungi regulates pH, soil organic matter turnover and nitrogen availability in acidic forest soils. Soil Biol Biochem 63:142–153. https://doi.org/10.1016/j.soilbio.2013.03.019
16. Clemmensen KE, Finlay RD, Dahlberg A, Stenlid J, Wardle DA, Lindahl BD (2015) Carbon sequestration is related to mycorrhizal fungal community shifts during long-term succession in boreal forests. New Phytol 205:1525–1536. https://doi.org/10.1111/nph.13208
17. Creutzig F, Roy J, Lamb WF, Azevedo IML, Bruin WBD, Dalkmann H, Edelenbosch OY, Geels FW, Grubler A, Hepburn C, Hertwich EG, Khosla R, Mattauch L, Minx JC, Ramakrishnan A, Rao ND, Steinberger JK, Tavoni M, Ürge-Vorsatz D, Weber EU (2018) Towards demand-side solutions for mitigating climate change. Nat Clim Change 8:260–263. https://doi.org/10.1038/s41558-018-0121-1
18. Davis MR, Condron LM (2002) Impact of grassland afforestation on soil carbon in New Zealand: a review of paired-site studies. Aust J Soil Res 40:675–690. https://doi.org/10.1071/SR01074
19. Deng SP, Tabatabai MA (1994) Cellulase activity of soils. Soil Biol Biochem 26:1347–1354. https://doi.org/10.1016/0038-0717(94)90216-X

20. Dick RP (2011) Methods of soil enzymology. Soil Science Society of America, Madison
21. Dijkstra FA, Smits MM (2002) Tree species effects on calcium cycling: The role of calcium uptake in deep soils. Ecosystems 5:385–398. https://doi.org/10.1007/s10021-001-0082-4
22. Dominguez DC (2004) Calcium signalling in bacteria. Mol Microbiol 54:291–297. https://doi.org/10.1111/j.1365-2958.2004.04276.x
23. Don A, Rebmann C, Kolle O, Scherer-Lorenzen M, Schulze E (2009) Impact of afforestation-associated management changes on the carbon balance of grassland. Glob Change Biol 15:1990–2002. https://doi.org/10.1111/j.1365-2486.2009.01873.x
24. Dungait JAJ, Hopkins DW, Gregory AS, Whitmore AP (2012) Soil organic matter turnover is governed by accessibility not recalcitrance. Glob Change Biol 18:1781–1796. https://doi.org/10.1111/j.1365-2486.2012.02665.x
25. Eivazi F, Tabatabai MA (1988) Glucosidases and galactosidases in soils. Soil Biol Biochem 20:601–606. https://doi.org/10.1016/0038-0717(88)90141-1
26. Fan X, Gao D, Zhao C, Wang C, Qu Y, Zhang J, Bai E (2021) Improved model simulation of soil carbon cycling by representing the microbially derived organic carbon pool. ISME J 15:2248–2263. https://doi.org/10.1038/s41396-021-00914-0
27. FAO (2020) Global Forest Resources Assessment 2020, main report. Food and Agriculture Organization of the United Nations, Rome
28. Friggens NL, Hester AJ, Mitchell RJ, Parker TC, Subke J, Wookey PA (2020) Tree planting in organic soils does not result in net carbon sequestration on decadal timescales. Glob Change Biol 26:5178–5188. https://doi.org/10.1111/gcb.15229
29. Guo LB, Gifford RM (2002) Soil carbon stocks and land use change: a meta analysis. Glob Change Biol 8:345–360. https://doi.org/10.1046/j.1354-1013.2002.00486.x
30. Haddix ML, Gregorich EG, Helgason BL, Janzen H, Ellert BH, Cotrufo MF (2020) Climate, carbon content, and soil texture control the independent formation and persistence of particulate and mineral-associated organic matter in soil. Geoderma 363:114160. https://doi.org/10.1016/j.geoderma.2019.114160
31. Hiltbrunner D, Zimmermann S, Hagedorn F (2013) Afforestation with Norway spruce on a subalpine pasture alters carbon dynamics but only moderately affects soil carbon storage. Biogeochemistry 115:251–266. https://doi.org/10.1007/s10533-013-9832-6
32. Hong S, Yin G, Piao S, Dybzinski R, Cong N, Li X, Wang K, Peñuelas J, Zeng H, Chen A (2020) Divergent responses of soil organic carbon to afforestation. Nat Sustain 3:694–700. https://doi.org/10.1038/s41893-020-0557-y
33. Hu Y, Zeng D, Fan Z, Chen G, Zhao Q, Pepper D (2008) Changes in ecosystem carbon stocks following grassland afforestation of semiarid sandy soil in the southeastern Keerqin Sandy Lands, China. J Arid Environ 72:2193–2200. https://doi.org/10.1016/j.jaridenv.2008.07.007
34. Huang Z, Davis MR, Condron LM, Clinton PW (2011) Soil carbon pools, plant biomarkers and mean carbon residence time after afforestation of grassland with three tree species. Soil Biol Biochem

43:1341–1349. https://doi.org/10.1016/j.soilbio.2011.03.008

35. Jia W, Li F, Dong L, Zhao X (2012) Carbon density and storage for *Pinus sylvestris* var *mongolica* plantation based on compatible biomass models. J Beijing For Univ 34:6–13. https://doi.org/10.13332/j.1000-1522.2012.01.018
36. Jobbágy EG, Jackson RB (2003) Patterns and mechanisms of soil acidification in the conversion of grasslands to forests. Biogeochemistry 64:205–229. https://doi.org/10.1023/A:1024985629259
37. Jobbágy EG, Jackson RB (2004) The uplift of soil nutrients by plants: Biogeochemical consequences across scales. Ecology 85:2380–2389. https://doi.org/10.1890/03-0245
38. Kallenbach CM, Frey SD, Grandy AS (2016) Direct evidence for microbial-derived soil organic matter formation and its ecophysiological controls. Nat Commun 7:13630. https://doi.org/10.1038/ncomms13630
39. Kirk PL (1950) Kjeldahl method for total nitrogen. Anal Chem 22:354–358. https://doi.org/10.1021/ac60038a038
40. Kleber M, Bourg IC, Coward EK, Hansel CM, Myneni SCB, Nunan N (2021) Dynamic interactions at the mineral-organic matter interface. Nat Rev Earth Environ 2:402–421. https://doi.org/10.1038/s43017-021-00162-y
41. Lal R (2004) Soil carbon sequestration to mitigate climate change. Geoderma 123:1–22. https://doi.org/10.1016/j.geoderma.2004.01.032
42. Lavallee JM, Soong JL, Cotrufo MF (2020) Conceptualizing soil organic matter into particulate and mineral-associated forms to address global change in the 21st century. Glob Change Biol 26:261–273. https://doi.org/10.1111/gcb.14859
43. Lefroy RDB, Blair GJ, Strong WM (1993) Changes in soil organic-matter with cropping as measured by organic-carbon fractions and ^{13}C natural isotope abundance. Plant Soil 155:399–402. https://doi.org/10.1007/BF00025067
44. Liang C, Amelung W, Lehmann J, Kästner M (2019) Quantitative assessment of microbial necromass contribution to soil organic matter. Glob Change Biol 25:3578–3590. https://doi.org/10.1111/gcb.14781
45. Liang C, Schimel JP, Jastrow JD (2017) The importance of anabolism in microbial control over soil carbon storage. Nat Microbiol 2:17105. https://doi.org/10.1038/nmicrobiol.2017.105
46. Lin G, Gao M, Zeng D, Fang Y (2020) Aboveground conservation acts in synergy with belowground uptake to alleviate phosphorus deficiency caused by nitrogen addition in a larch plantation. For Ecol Manage 473:118309. https://doi.org/10.1016/j.foreco.2020.118309
47. Liu Y, Wang A, An Y, Lian P, Wu D, Zhu J, Meinzer FC, Hao G (2018) Hydraulics play an important role in causing low growth rate and dieback of aging *Pinus sylvestris* var. *mongolica* trees in plantations of Northeast China. Plant Cell Environ 41:1500–1511. https://doi.org/10.1111/pce.13160
48. Lugato E, Lavallee JM, Haddix ML, Panagos P, Cotrufo MF (2021) Different climate sensitivity of particulate and mineral-associated soil organic matter. Nat Geosci 14:295–300.

https://doi.org/10.1038/s41561-021-00744-x

49. Martens DA, Reedy TE, Lewis DT (2004) Soil organic carbon content and composition of 130-year crop, pasture and forest land-use managements. Glob Change Biol 10:65–78. https://doi.org/10.1046/j.1529-8817.2003.00722.x
50. Neumann-Cosel L, Zimmermann B, Hall JS, van Breugel M, Elsenbeer H (2011) Soil carbon dynamics under young tropical secondary forests on former pastures–A case study from Panama. For Ecol Manage 261:1625–1633. https://doi.org/10.1016/j.foreco.2010.07.023
51. Ortiz C, Vázquez E, Rubio A, Benito M, Schindlbacher A, Jandl R, Butterbach-Bahl K, Diaz-Pinés E (2016) Soil organic matter dynamics after afforestation of mountain grasslands in both a Mediterranean and a temperate climate. Biogeochemistry 131:267–280. https://doi.org/10.1007/s10533-016-0278-5
52. Poeplau C, Don A (2013) Sensitivity of soil organic carbon stocks and fractions to different land-use changes across Europe. Geoderma 192:189–201. https://doi.org/10.1016/j.geoderma.2012.08.003
53. Prescott CE, Vesterdal L (2021) Decomposition and transformations along the continuum from litter to soil organic matter in forest soils. For Ecol Manage 498:119522. https://doi.org/10.1016/j.foreco.2021.119522
54. Richter DD, Markewitz D, Trumbore SE, Wells CG (1999) Rapid accumulation and turnover of soil carbon in a re-establishing forest. Nature 400:56–58. https://doi.org/10.1038/21867
55. Rosseel Y (2012) lavaan: an R package for structural equation modeling. J Stat Softw 48:1–36. https://doi.org/10.18637/jss.v048.i02
56. Rowley MC, Grand S, Verrecchia ÉP (2018) Calcium-mediated stabilisation of soil organic carbon. Biogeochemistry 137:27–49. https://doi.org/10.1007/s10533-017-0410-1
57. Shao S, Zhao Y, Zhang W, Hu G, Xie H, Yan J, Han S, He H, Zhang X (2017) Linkage of microbial residue dynamics with soil organic carbon accumulation during subtropical forest succession. Soil Biol Biochem 114:114–120. https://doi.org/10.1016/j.soilbio.2017.07.007
58. Shi S, Zhang W, Zhang P, Yu Y, Ding F (2013) A synthesis of change in deep soil organic carbon stores with afforestation of agricultural soils. For Ecol Manage 296:53–63. https://doi.org/10.1016/j.foreco.2013.01.026
59. Sokol NW, Sanderman J, Bradford MA (2019) Pathways of mineral-associated soil organic matter formation: Integrating the role of plant carbon source, chemistry, and point of entry. Glob Change Biol 25:12–24. https://doi.org/10.1111/gcb.14482
60. Terrer C, Phillips RP, Hungate BA, Rosende J, Pett-Ridge J, Craig ME, van Groenigen KJ, Keenan TF, Sulman BN, Stocker BD, Reich PB, Pellegrini AFA, Pendall E, Zhang H, Evans RD, Carrillo Y, Fisher JB, Van Sundert K, Vicca S, Jackson RB (2021) A trade-off between plant and soil carbon storage under elevated CO_2. Nature 591:599–603. https://doi.org/10.1038/s41586-021-03306-8
61. Tong X, Brandt M, Yue Y, Horion S, Wang K, Keersmaecker WD, Tian F, Schurgers G, Xiao X, Luo Y, Chen C, Myneni R, Shi Z, Chen H, Fensholt R (2018) Increased vegetation growth and carbon stock in

China karst via ecological engineering. Nat Sustain 1:44–50. https://doi.org/10.1038/s41893-017-0004-x

62. Wang F, Zhu W, Chen H (2016) Changes of soil C stocks and stability after 70-year afforestation in the Northeast USA. Plant Soil 401:319–329. https://doi.org/10.1007/s11104-015-2755-3
63. Wang S, Huang Y (2020) Determinants of soil organic carbon sequestration and its contribution to ecosystem carbon sinks of planted forests. Glob Change Biol 26:3163–3173. https://doi.org/10.1111/gcb.15036
64. Wiesmeier M, Dick DP, Rumpel C, Dalmolin RSD, Hilscher A, Knicker H (2009) Depletion of soil organic carbon and nitrogen under *Pinus taeda* plantations in Southern Brazilian grasslands (*Campos*). Eur J Soil Sci 60:347–359. https://doi.org/10.1111/j.1365-2389.2009.01119.x
65. Witzgall K, Vidal A, Schubert DI, Höschen C, Schweizer SA, Buegger F, Pouteau V, Chenu C, Mueller CW (2021) Particulate organic matter as a functional soil component for persistent soil organic carbon. Nat Commun 12:4115. https://doi.org/10.1038/s41467-021-24192-8
66. Xu H, Qu Q, Chen Y, Liu G, Xue S (2021) Responses of soil enzyme activity and soil organic carbon stability over time after cropland abandonment in different vegetation zones of the Loess Plateau of China. CATENA 196:104812. https://doi.org/10.1016/j.catena.2020.104812
67. Yang B, Qi K, Bhusal DR, Huang J, Chen W, Wu Q, Hussain A, Pang X (2020) Soil microbial community and enzymatic activity in soil particle-size fractions of spruce plantation and secondary birch forest. Eur J Soil Biol 99:103196. https://doi.org/10.1016/j.ejsobi.2020.103196
68. Zhang Q, Jia X, Wei X, Shao M, Li T, Yu Q (2020) Total soil organic carbon increases but becomes more labile after afforestation in China's Loess Plateau. For Ecol Manage 461:117911. https://doi.org/10.1016/j.foreco.2020.117911
69. Zhang X, Zhang X, Han H, Shi Z, Yang X (2019) Biomass accumulation and carbon sequestration in an age-sequence of Mongolian pine plantations in Horqin sandy land, China. Forests 10:197. https://doi.org/10.3390/f10020197

Figures

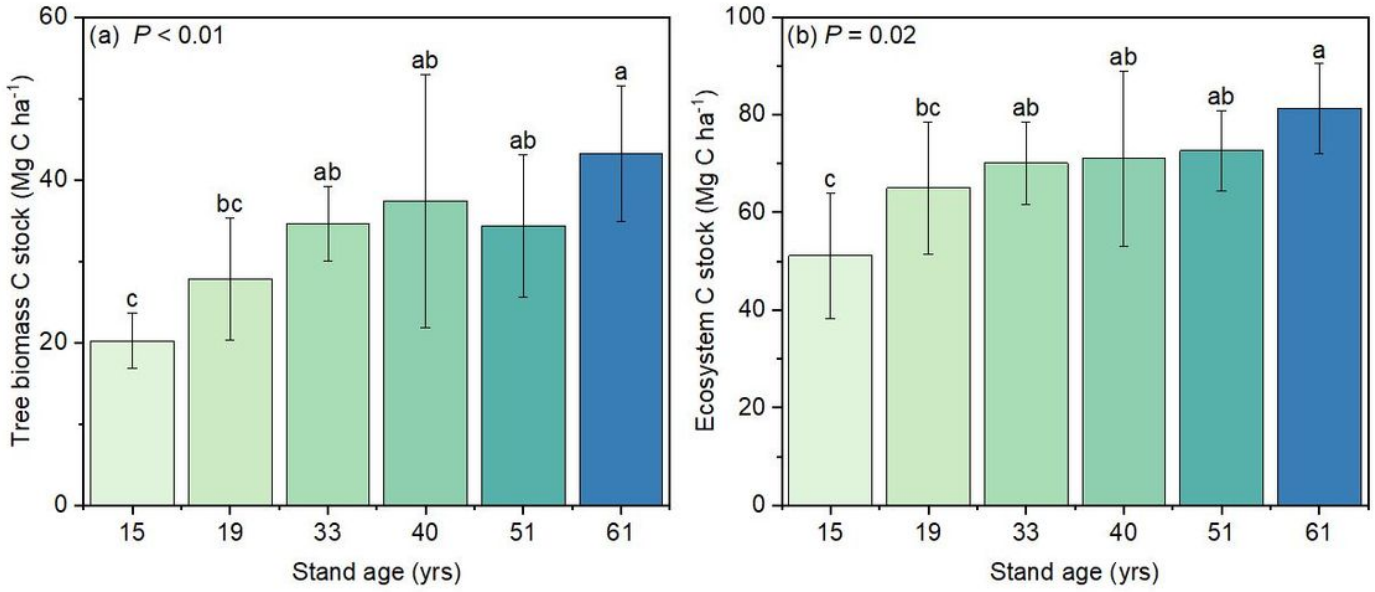

Figure 1

Changes in C stocks of tree biomass (a) and ecosystem (b) along a chronosequence of Mongolian pine plantations (mean ± SD, *n* = 5). Different lowercase letters indicate significant differences among stand ages.

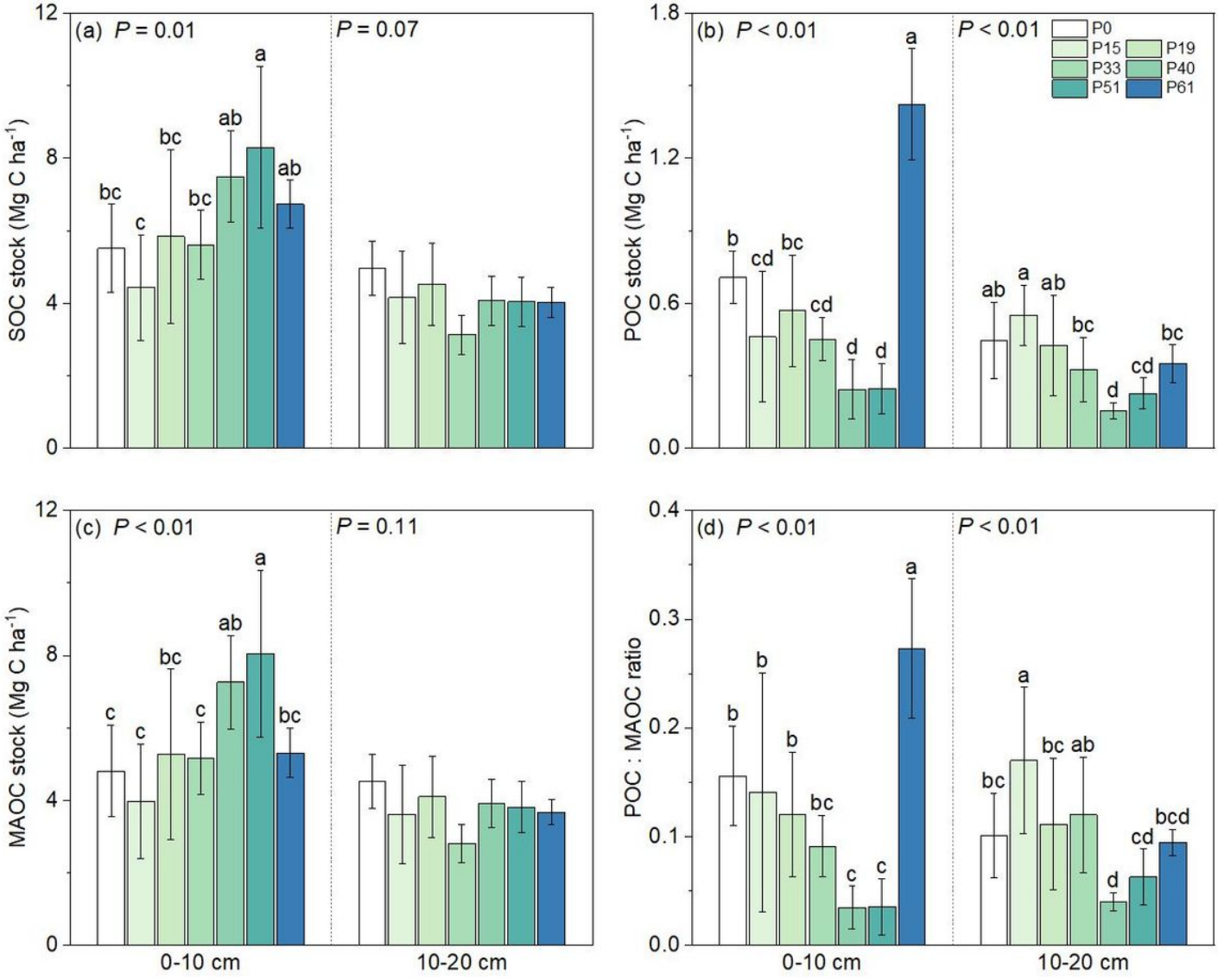

Figure 2

Changes in soil organic C (SOC) stock (a), particulate organic C (POC) stock (b), mineral-associated organic C (MAOC) stock (c) and POC:MAOC ratio (d) of the 0–10 and 10–20 cm soil layers along a chronosequence of Mongolian pine plantations (mean ± SD, *n* = 5). Different lowercase letters indicate significant differences among stand ages. P0, P15, P19, P33, P40, P51 and P61 separately represent sandy grasslands, 15-, 19-, 33-, 40-, 51- and 61-year-old Mongolian pine plantations.

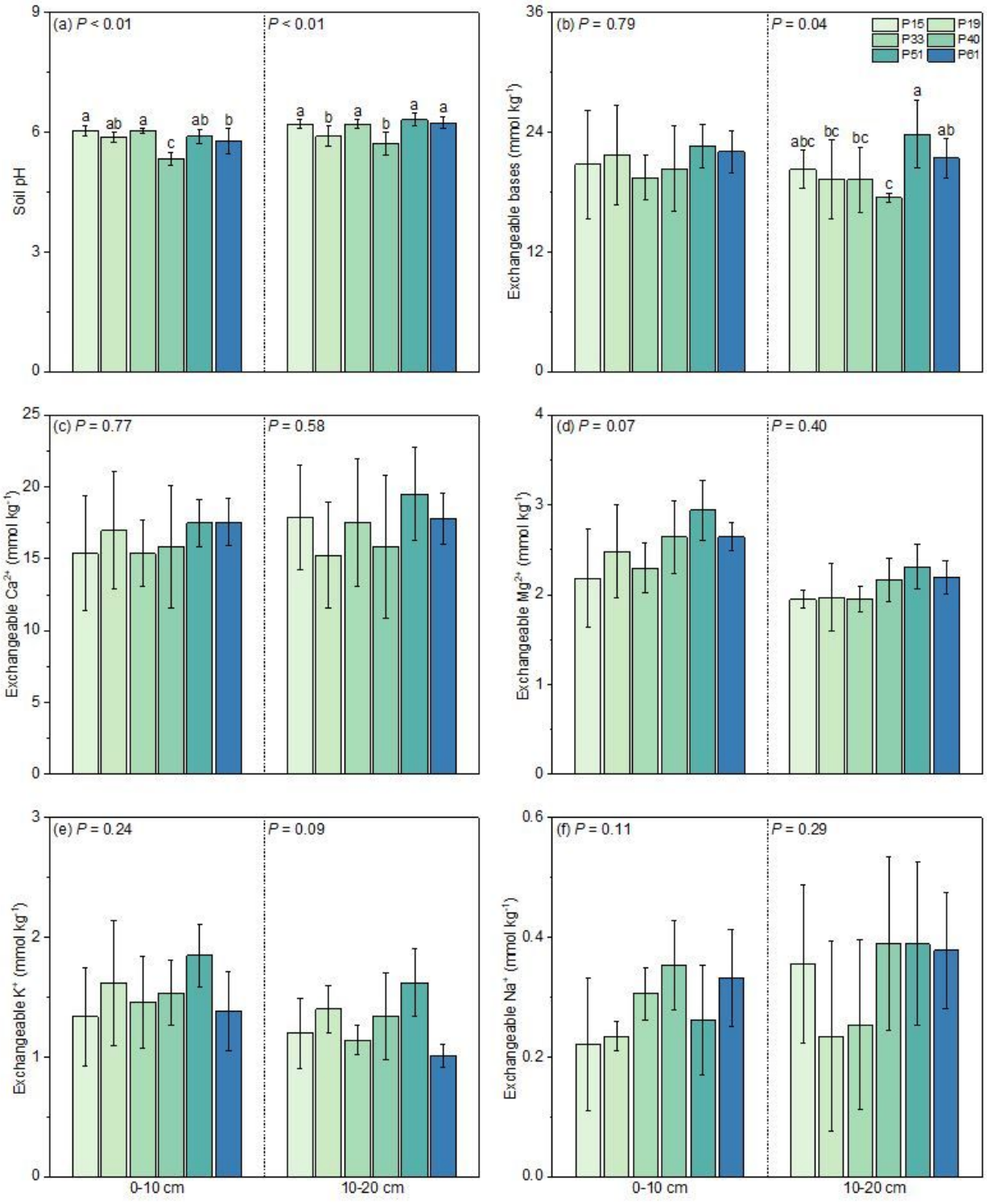

Figure 3

Changes in soil acid-base chemical variables of the 0–10 and 10–20 cm soil layers along a chronosequence of Mongolian pine plantations (mean ± SD, n = 5). Different lowercase letters indicate significant differences among stand ages. Exchangeable bases are the sum of exchangeable Ca^{2+}, Mg^{2+}, K^{+} and Na^{+} concentrations. P15, P19, P33, P40, P51 and P61 separately represent 15-, 19-, 33-, 40-, 51- and 61-year-old Mongolian pine plantations

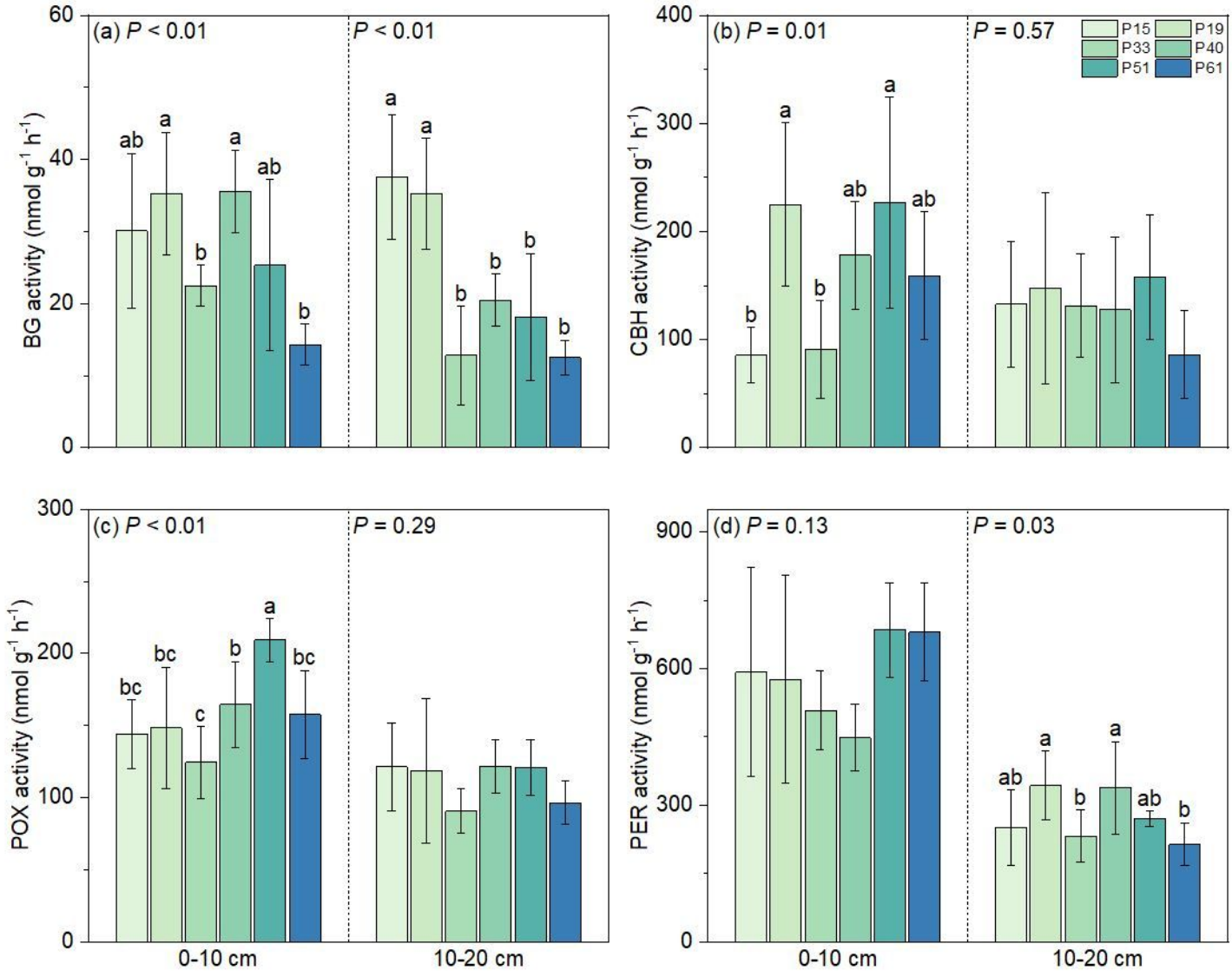

Figure 4

Changes in potential activities of β-1,4-glucosidase (BG, a), cellobiohydrolase (CBH, b), phenol oxidase (POX, c) and peroxidase (PER, d) of the 0–10 and 10–20 cm soil layers along a chronosequence of Mongolian pine plantations (mean ± SD, *n* = 5). Different lowercase letters indicate significant differences among stand ages. P15, P19, P33, P40, P51 and P61 separately represent 15-, 19-, 33-, 40-, 51- and 61-year-old Mongolian pine plantations

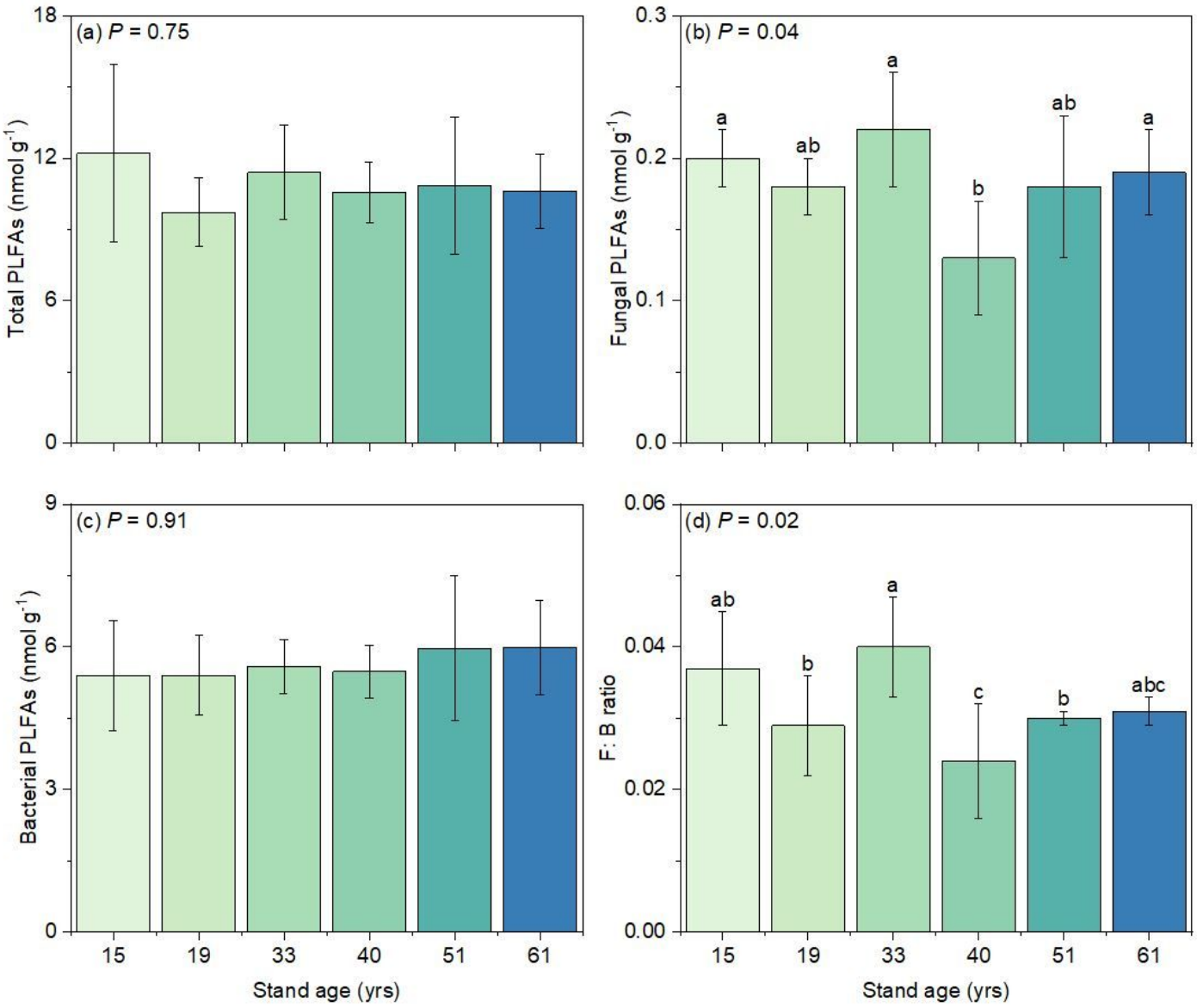

Figure 5

Changes in total phospholipid fatty acids (PLFAs, a), fungal PLFAs (b), bacterial PLFAs (c), F:B ratio (d) of the 0–10 cm soil layer along a chronosequence of Mongolian pine plantations (mean ± SD, *n* = 5). F:B ratio, the ratio of fungal PLFAs to bacterial PLFAs. Different lowercase letters indicate significant differences among stand ages.

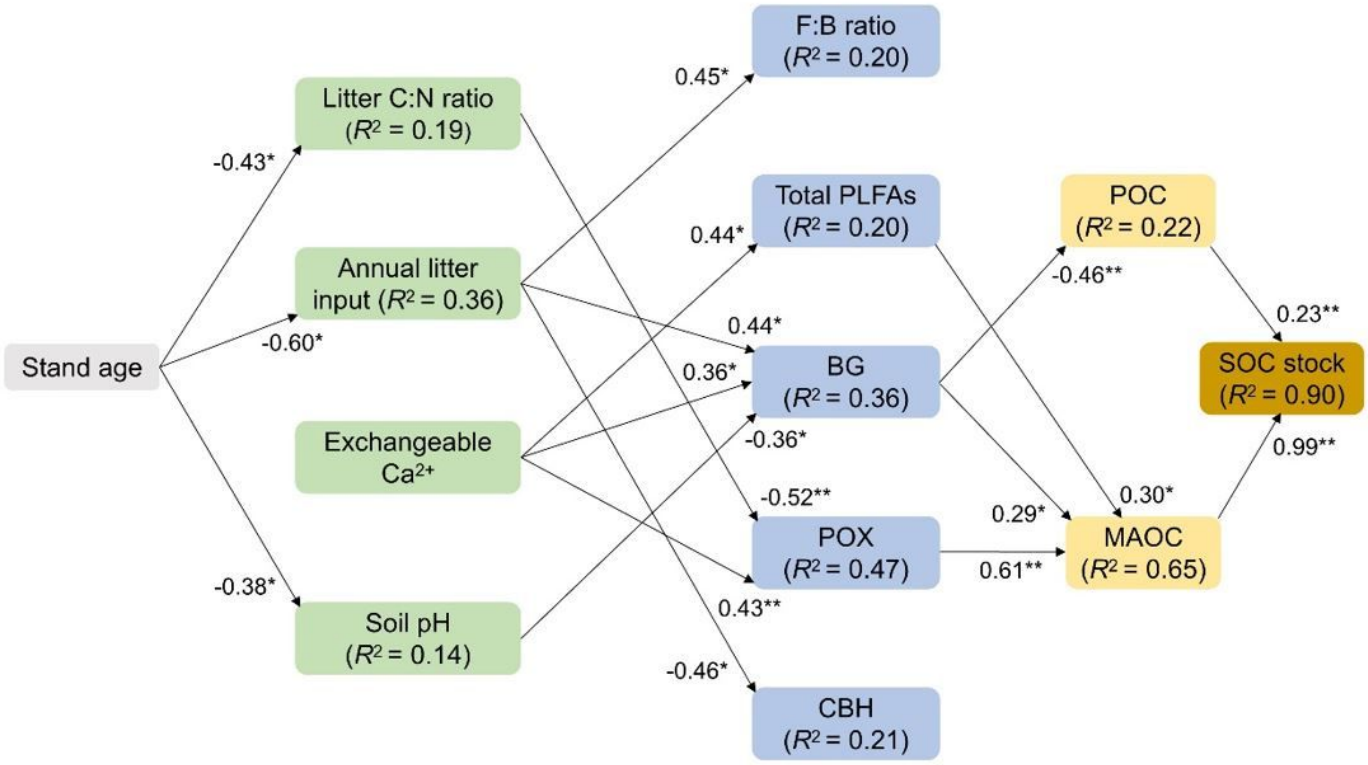

Figure 6

Final structural equation model depicting direct and indirect effects of stand ages, litter quality and quantity, soil acid-base chemistry, soil microbial properties, and C fractions on SOC stocks in the 0–10 cm soil layer. Numbers next to arrows indicate standardized path coefficients. R^2 represents the percentage of variation explained by all paths. PLFA, phospholipid fatty acid; F:B ratio, the ratio of fungal PLFAs to bacterial PLFAs; BG, β-1,4-glucosidase; CBH, cellobiohydrolase; POX, phenol oxidase; POC, particulate organic C; MAOC, mineral-associated organic C; *, P <0.05; **, P <0.01

Supplementary Files

This is a list of supplementary files associated with this preprint. Click to download.

- Supportinginformation.docx